

Model-Based Edge Reconstruction for Low Bit-Rate Wavelet-Compressed Images

Guoliang Fan, *Student Member, IEEE*, and Wai-Kuen Cham, *Senior Member, IEEE*

Abstract—At low bit rates, wavelet-based image coding is superior to most traditional block-based methods in terms of visibility and severity of coding artifacts in coded images. However, the compressed images still suffer from obvious distortions around sharp edges, which are perceptually objectionable. In order to improve image quality for low bit-rate wavelet-based image coding, we proposed a model-based edge-reconstruction algorithm for recovering the lossy edges in coded images. Our approach applies a general model to represent varieties of edges existing in an image. Based on this model, the edge degradation process due to quantization errors of wavelet coefficients is analyzed with the characterization of two kinds of artifacts at edges. We develop two operations, model-based edge approximation and Gaussian smoothing, to reconstruct distorted edges by reducing both artifacts respectively. The proposed method is able to improve image quality in terms of both visual perception and image fidelity (peak signal-to-noise ratio) for most images coded by wavelet-based methods at low bit-rates.

Index Terms—Edge model, edge reconstruction, image coding, image processing, post-processing, wavelet transform.

I. INTRODUCTION

IMAGE compression is aimed to minimize the number of bits needed to represent an image while maintaining sufficient image quality. Images coded at low bit-rates suffer from the loss of details and sharpness, as well as various coding artifacts. On the other hand, with the increasing needs of image transmission and storage, the demand for higher compression is also increasing. This problem can be alleviated by effective post-processing techniques, which are able to improve the coding efficiency and, at the same time, maintain the compatibility with the existing encoder and decoder. Since different methods have different artifacts, the design of post-processing should be tailored for a coding method. For block-based discrete cosine transform (DCT) coding, the quality of low bit-rate compressed images is degraded mainly by the “blocking effects” across the block boundaries and the “ringing effects” around sharp edges. Due to the widespread use of DCT-based image coding, many post-processing schemes have been developed, among which most techniques attempt to remove the blocking effect [1]–[5], and some methods focus on the suppression of the ringing effect [6] or both artifacts [7]–[10].

Manuscript received March 6, 1998; revised July 17, 1999. This paper was recommended by Associate Editor W. Li.

G. Fan was with the Department of Electronic Engineering, The Chinese University of Hong Kong, Hong Kong. He is now with the Department of Electrical and Computer Engineering, University of Delaware, Newark, DE 19716 USA.

W.-K. Cham is with the Department of Electronic Engineering, The Chinese University of Hong Kong, Hong Kong.

Publisher Item Identifier S 1051-8215(00)01640-2.

Recently, wavelet transforms have attracted considerable attention with their application to image coding [11]–[14] due to their unique space–frequency characteristics. Moreover, the hierarchical wavelet image representation also allows efficient quantization strategies, such as zero-tree quantization [11]–[13], for exploiting the spatial and frequency characteristics of wavelet coefficients. In particular, at low bit-rates (e.g., below 0.25 bits per pixel (bpp) for highly detailed gray-scale images), wavelet-based image coding demonstrates some advantages over the traditional block-based methods in terms of visibility and severity of coding artifacts in compressed images. However, the coded images still bear obvious artifacts among continuous regions and around sharp edges as a result of the considerable quantization errors of wavelet coefficients. The quantization errors in high-frequency subbands generally result in ringing effects, as well as blurring effects near sharp edges [15], and those in both low-frequency and high-frequency subbands cause ripples or blotchiness in smooth regions [16].

In order to attain sufficient image quality for low bit-rate wavelet-based image coding, post-processing is an efficient technique for improving compression results at low bit-rates. Though some efforts have been made to improve continuousness of smooth regions in the coded images [16], little work has been devoted to the edge recovery, which is more needful for low bit-rate wavelet-based image coding. Since edges define the most recognizable features for objects in an image, the distortions around edges are disturbing and annoying to human perception. For DCT-based image coding, the ringing effect is considered the major artifact around edges. Thus, some methods based on edge-preserving maximum *a posteriori* (MAP) estimation [4], [7], [10], or adaptive filtering [6], [9], [17] were proposed to cope with this problem. However, besides the ringing effect, edges have also been blurred by the low pass filtering effect introduced by the allocation of zero bit to high-frequency coefficients. The previous techniques for reducing the ringing effect cannot eliminate the blurring effects and are unable to reproduce the edge sharpness.

The objective of post-processing is to improve image quality, which can be achieved by image enhancement or image restoration. The former is concerned with improving image visual quality by accentuating some image features without considering image fidelity [peak signal-to-noise ratio (PSNR)], and the latter tries to recover the original signal from the degraded one by means of a model for signal or a model for the degradation process. Comparatively speaking, image restoration is more useful in the case of image compression where the fidelity of the compressed image is still of main concern. However, the effective image restoration of compressed image

may be difficult for the unknown of degradation model of image coding, and even with the known degradation process, the ill-posed or non-unique inversion process may make restoration impossible or computational intensive [18]. Previous post-processing techniques [1], [4], [5], [16] with image restoration formulation share some characteristics.

- 1) There are no explicit or deterministic characterization of the degradation process.
- 2) Edge deblurring is seldom taken into consideration.
- 3) The solution of problem involves iteration operations which require intensive computation.

On the other hand, at low bit-rates, image enhancement is somewhat necessary and helpful for human perception [19], [20]. Some post-processing techniques contain elements of both restoration and enhancement, but very few provide the flexibility to allow a tradeoff between them for the reconstructed image.

In this paper, we propose a novel post-processing method for low bit-rate wavelet-based image coding for edge reconstruction. Edge reconstruction can be accomplished in spatial domain or transform domain. In [21], the edge reconstruction for image interpolation is performed in the wavelet transform domain by extrapolating the wavelet coefficients according to the decaying model of a step edge. The proposed approach operates in spatial domain and reconstructs distorted edges by the use of a deterministic edge model [22]. Based on this model, the degradation process of edges due to wavelet-based image coding using zero-tree quantization was analyzed. We developed a new edge model for coded images by the introduction of two new terms to the original edge model, which is able to characterize two artifacts, ringing effects and blurring effects, around lossy edges. The problem of edge reconstruction is formulated as that of image restoration and can be solved by recovering original edge structure and reducing quantization noise. The former involves estimating original model parameters from the coded signal. The latter is implemented by local Gaussian filtering of edges in the coded signal. Furthermore, we introduce a parametric reconstruction model which is able to provide a flexible tradeoff between visual enhancement and fidelity improvement for the reconstructed image. Compared with previous post-processing techniques, the proposed approach has the advantage of low computation complexity because it can be implemented straightforwardly, without any iteration operation.

This paper is organized as follows. Based on an edge model, we analyze the degradation process of edges due to wavelet-based coding in Section II. Section III discusses the proposed edge reconstruction algorithm. The experimental results are presented in Section IV. Finally, we draw conclusions in Section V.

II. EDGE ANALYSIS

In an image, edges carry important information which usually reflects abrupt luminance changes and irregular structures. There are two primitives for characterizing edges which are the edge curves, i.e., the loci of edge points, and the variation of the image surface within the narrow strips along edge curves. The former can be obtained by edge detection followed by an associated linking scheme. The latter can be established by mod-

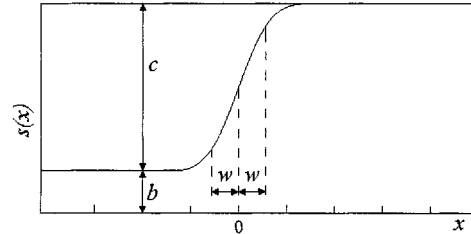


Fig. 1. 1-D edge model with edge center at $x = 0$.

eling edges in the real signal with an idealized function which can be parameterized efficiently in order to represent the edges of various conformations. Though an edge model may not precisely reflect the real variations, it will provide us a controllable approximation by which the problem of edge-related processing can be formulated and analyzed. We will introduce an edge model image based on which the edge degradation due to image compression is discussed

A. Edge Model in Original Images

The edge model adopted here has been described in depth by Van Beek in [22]. Some basic formulation and operation related to the edge model are briefly presented as follows.

Edges in two-dimensional (2-D) images have local one-dimensional (1-D) structure features, in that there are sharp intensity changes in one direction together with little or no change in the perpendicular direction. Hence, most descriptions of the edge model in this paper are based on the 1-D form. With some assumptions, an edge $s(x)$ at $x = 0$ is modeled as the *Gaussian smoothed step edge* defined by

$$s(x) \equiv s(x; b, c, w) = h(x; b, c) * g(x; w) \quad (1)$$

where

$$h(x; b, c) = b + cU(x) \quad (2)$$

and

$$g(x; w) = \frac{1}{\sigma\sqrt{2\pi}} \exp\left(-\frac{x^2}{2\sigma^2}\right), \quad \text{with } \sigma = w. \quad (3)$$

From (1)–(3), an edge can be represented as

$$s(x; b, c, w) = b + \frac{c}{2} \left(1 + \operatorname{erf}\left(\frac{x}{w\sqrt{2}}\right)\right) \quad (4)$$

where $\operatorname{erf}(\cdot) \in [-1, 1]$ is a scaled error function, w the parameter controlling the width of the edge, c the contrast across the edge, and b the intensity at the base of the edge. These parameters are depicted in Fig. 1. In order to model edges in one signal, we need to conduct edge detection and model-parameter estimation as follows.

B. Edge Detection and Parameter Estimation

Canny edge detection [23] is used by convolving the signal $s(x)$ with the derivative of a Gaussian function $g'_d(x; \sigma_d)$, where σ_d controls the correctness of edge detection and the accuracy

of edge localization. Without considering the noise, the model output of edge detection is

$$\begin{aligned} d(x; w, c, \sigma_d) &= s(x; b, c, w) * g'_d(x; \sigma_d) \\ &= c \cdot g(x; \sigma_1) \end{aligned} \quad (5)$$

with $\sigma_1 = \sqrt{w^2 + \sigma_d^2}$. An edge point is identified by checking out local maximum in the magnitude of the response.

In [22], the response of edge detection is also applied for estimating the model parameters of a detected edge. Given the response of edge detection expressed in (5) whose local maximum is recognized as an edge, the detected edge may not be at the true position because of the discretization of the signal. "Edge point" will denote the edge on the sampled grid of the discrete signal and "edge center" will denote the true position of the edge in the continuous version. Edge points can be identified during edge detection as shown in (5). For a signal $s_0(x)$ with unit sampling interval, if the edge point is at $x = 0$ and the true edge center is at $x = x_0$ ($|x_0| < 0.5$), i.e.,

$$s_0(x) = s(x - x_0; b, c, w) \quad (6)$$

then (5) becomes

$$d(x; w, c, \sigma_1) = s_0(x) * g'_d(x; \sigma_d) = c \cdot g(x - x_0; \sigma_1). \quad (7)$$

By sampling (7) at $x = -a, 0$, and a , three measurements can be obtained as follows:

$$\begin{aligned} d_1 \equiv d(0; c, w, \sigma) &= \frac{c}{\sqrt{2\pi(w^2 + \sigma_d^2)}} \\ &\cdot \exp\left(-\frac{x_0^2}{2(w^2 + \sigma_d^2)}\right) \end{aligned} \quad (8)$$

$$\begin{aligned} d_2 \equiv d(a; c, w, \sigma) &= \frac{c}{\sqrt{2\pi(w^2 + \sigma_d^2)}} \\ &\cdot \exp\left(-\frac{(a - x_0)^2}{2(w^2 + \sigma_d^2)}\right) \end{aligned} \quad (9)$$

$$\begin{aligned} d_3 \equiv d(-a; c, w, \sigma) &= \frac{c}{\sqrt{2\pi(w^2 + \sigma_d^2)}} \\ &\cdot \exp\left(-\frac{(-a - x_0)^2}{2(w^2 + \sigma_d^2)}\right). \end{aligned} \quad (10)$$

From (4), (8)–(10), where $a = 1$ is a practical choice in the sampled 1-D signal, parameter c , w , b and the subpixel position of the edge center can be estimated using three outputs near the peak of (7) as follows:

$$w^2 = \frac{a^2}{\ln\left(\frac{d_1 d_1}{d_2 d_3}\right)} - \sigma_d^2 \quad (11)$$

$$x_0 = \frac{a \ln(d_2/d_3)}{2 \ln\left(\frac{d_1 d_1}{d_2 d_3}\right)} \quad (12)$$

$$c \approx d_1 \sqrt{\frac{2\pi a^2}{\ln\left(\frac{d_1 d_1}{d_2 d_3}\right)}} \left(\frac{d_2}{d_3}\right)^{1/4a} \quad (13)$$

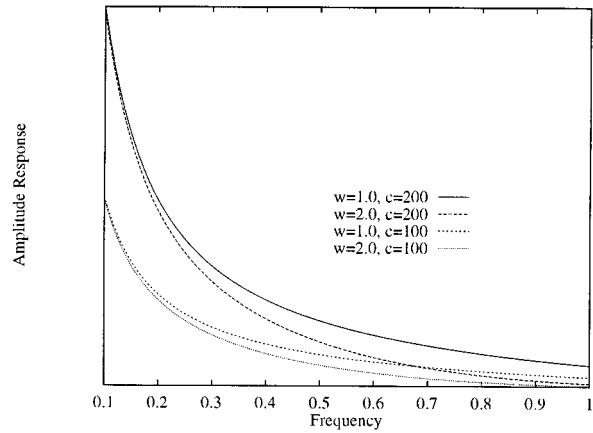


Fig. 2. Amplitude response of the 1-D edge model.

$$b = s_0(x_0) - \frac{c}{2}. \quad (14)$$

In a discrete signal, $s(x_0)$ can be obtained by linear interpolation between the two nearest sampled points.

It is shown in [22] for most well-acquisitioned natural images, the majority of edges has width w ranging from 0.5 to 1.5. With the consideration of various errors, the setting of $\sigma_d = 1.0$ is a reasonable value in the case of original images. The 2-D edge model and relevant analysis can be shaped into the 1-D model framework discussed above. Essentially, the 2-D edge model is operated in the 1-D way, thus the model-based characterization can be adapted to edges with various loci in the image.

This edge model was applied to image coding [22]. An image was represented by edges and their interpolation. An edge was characterized by three parameters of the edge model. Since many details in an image may not be precisely represented by the edge model, and the edge parameters were not coded effectively, the coding performance is not satisfactory. However, the coded images sustain good edge features. This implies that the edge model is effective for the representation of edge structures and edge reconstruction in distorted images.

C. Edge Degradation Due to Image Compression

We now analyze the edge-degradation process due to the quantization error of wavelet coefficients based on the considerations of the frequency properties of the edge signal $s(x)$ defined in (1) and the characteristics of zero-tree quantization. For simplicity, the problem is discussed in the 1-D continuous form and the results can be adapted to the 2-D discrete case. Denote the Fourier transform of $s(x)$ by

$$S(\omega_x) = \frac{c}{j\omega_x} e^{-(w^2 \omega_x^2 / 2)} + 2\pi \left(b + \frac{c}{2}\right) \delta(\omega_x)$$

where ω_x is the spatial frequency and $\delta(\cdot)$ the Dirac delta function. We show the amplitude responses $|S(\omega_x)|$ for edges with different model parameters in Fig. 2. From Fig. 2, it is observed that the amplitude response of the edge model decays with a rate related to w and c of the edge. Similar results can be obtained for discrete wavelet transform (DWT). In wavelet-based image coding, DWT decomposes an image over several scales

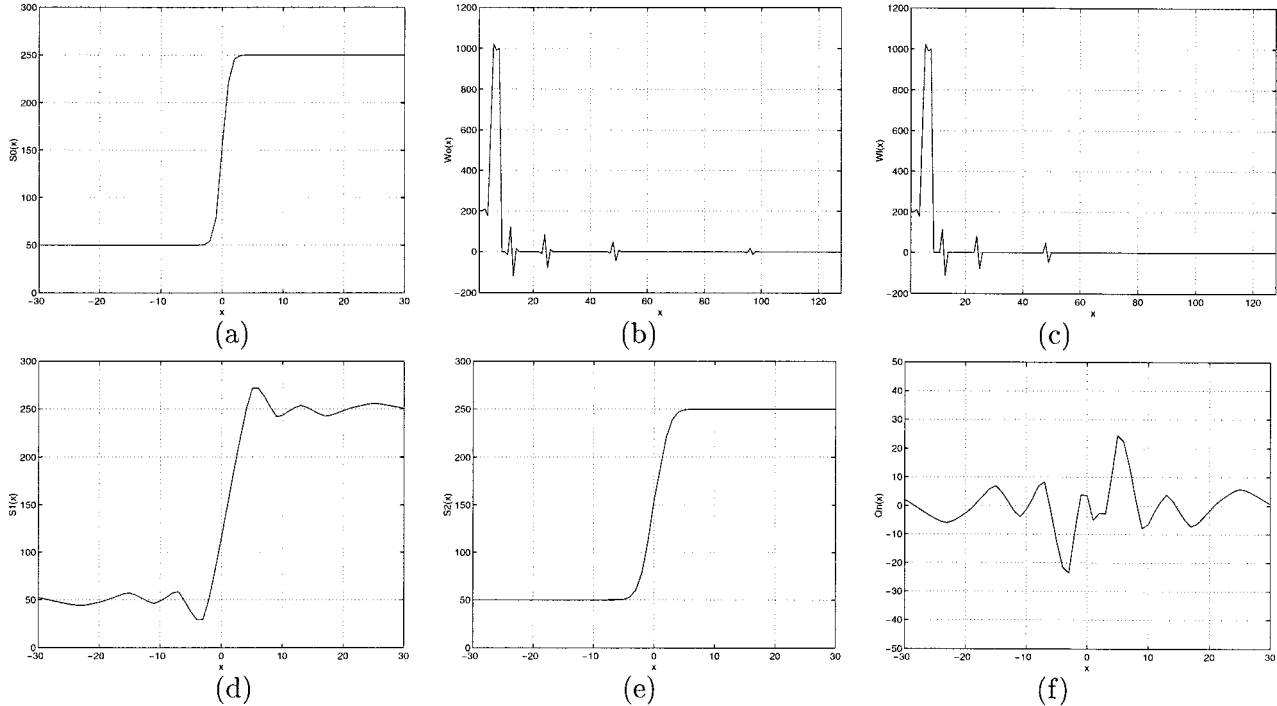


Fig. 3. Edge analysis with quantization error. (a) The original edge signal $s_0(x) = s(x - x_0; w, b, c)$ with $x_0 = 0$, $w = 1.0$, $b = 50$, and $c = 200$. (b) $w_{2^j}^0(u)$ ($j = 1, 2, 3, 4$), DWT of $s_0(x)$ over four scales. (c) $w_{2^j}^1(u)$, quantized version of $w_{2^j}^0(u)$ with quantization threshold $T_q = 64$. (d) $s_1(x)$, the coded version of $s_0(x)$. (e) $s_2(x) = s(x - x_0; \lambda w, b, c)$ with $\lambda = 1.85$, zero-phase low-pass filtering part in $s_1(x)$. (f) $q_n(x)$, the quantization noise in $s_1(x)$. (The signals $s_0(x)$ in (a), $s_1(x)$ in (d), $s_2(x)$ in (e), and $q_n(x)$ in (f) are depicted partially with $x \in [-30, 30]$.)

where most energy is compacted to the low-pass band with a small number of coefficients of large magnitude, and high-frequency components are dispersed among the high-frequency subbands with a large number of coefficients of small magnitude. Furthermore, zero-tree quantization of wavelet coefficients results in keeping the higher bits of larger coefficients and discarding smaller ones. Therefore, such a quantization scheme causes a considerable truncation of high-frequency energy, and introduces relatively little effect on low-frequency components. Thus, the wavelet coefficients in high-frequency subbands contributed to edges are normally of small magnitude and discarded during quantization. This is similar to the idealized low-pass filtering in the Fourier transform domain. It will result in blurring effect and ringing effect, which are also observed in wavelet-based image compression. Since the support of wavelet basis functions is compact, the ringing effects in a compressed image are locally distributed around edges. Based on these observations and analysis, we give the following formulation of edge degradation, in which edges in a compressed image is represented in the 1-D form.

Ideally speaking, we assume that during wavelet-based coding using zero-tree quantization, which is modulus thresholding after uniform quantization of wavelet coefficients, the original edge signal $s_0(x)$ of (6) is locally filtered with a low-pass zero-phase filter $f(x)$ of unity integral, accompanied with quantization noise $q_n(x)$ in the output. In our formulation, $f(x)$ is applied to characterizing blurring effect and $q_n(x)$ can correspond to the ringing effect in the compressed signal. We, therefore, propose to model the coded signal $s_1(x)$ by

$$s_1(x) = s(x - x_0; w, b, c) * f(x) + q_n(x). \quad (15)$$

Low-pass filter $f(x)$ widens w by a factor λ ($\lambda > 1$) which is related to the amount of high-frequency components truncated and the decaying rate of $|s(\omega_x)|$. From Fig. 2, we see that the same quantization threshold may result in different low-pass filtering effects on edges with different model parameters due to their different spectrum decaying rates. For simplicity, we only consider the effects on the parameter w . Intuitively, the width of the distorted edge should be proportional to the width of the original one. Hence, we use a multiplicative factor to characterize different edge widening influences of the low-pass filtering by $f(x)$. Experiments have been conducted, which showed that the multiplicative factor can produce images of slightly higher PSNR than an additive one.

If we assume that $f(x)$ is an FIR filter which has a symmetrical (about origin) impulse response of unity integral, it can be proved that the filtering of $s_0(x)$ by $f(x)$ leaves the position of the edge center x_0 unmoved, as well as the value of the edge center $s(x_0)$ unchanged, and causes no effect on c and b , so (15) can be rewritten in the form of

$$s_1(x) = s(x - x_0; w_1, b, c) + q_n(x) \quad (16)$$

where

$$w_1 = \lambda \cdot w. \quad (17)$$

In Fig. 3, we demonstrate above analysis through an example of a 1-D discrete edge signal $s_0(x) = s(x - x_0; w, b, c)$ which has 128 sampling points and edge model parameters $x_0 = 0$, $w = 1.0$, $b = 50$ and $c = 200$, as shown in Fig. 3(a). The wavelet transform of $s_0(x)$ over four scales, $w_{2^j}^0(x)$ ($j = 1, 2, 3, 4$), is given in Fig. 3(b), and a quantized

version with quantization threshold $T_q = 64$, $w_2^1(x)$, is shown in Fig. 3(c). Fig. 3(d) gives $s_1(x)$, the coded version of $s_0(x)$. According to (16), $s_1(x)$ can be decomposed into two components which are depicted in Fig. 3(e) and (f), respectively.

D. Edge Detection in the Compressed Signal

The response of edge detection using Canny detector for the coded signal $s_1(x)$ is expressed as

$$d_l(x) = s_1(x) * g'_d(x) = c \cdot g(x - x_0; w_2) + q_n(x) * g'_d(x) \quad (18)$$

where $w_2 = \sqrt{w_1^2 + \sigma_d^2}$. Thus, if the influence of quantization noise $q_n(x)$ is able to be suppressed by a suitable σ_d during edge detection, then the position of the local maximum in (18) will be the same as that in (7), which means that the lossy compression does not introduce shift to the original position of the edge point.

E. Model Parameter Estimation in the Compressed Signal

A two-step estimation is developed to estimate the original model parameters from the coded signal. First, the initial parameter estimation of signal $s_1(x)$ is obtained by (11) and (13) from the response of (18), and the estimated values of parameter c and w are denoted by \bar{c} and \bar{w} , respectively. Then, the parameter estimation of the original signal $s_0(x)$, where the computed values of model parameters c , b , and w are denoted by \hat{c} , \hat{b} and \hat{w} , respectively, is conducted as follows. In the compressed signal, the estimation of subpixel position x_0 in (15) is less meaningful due to the fact that the precision of multi-point estimation has been deteriorated by the lossy compression, especially at low bit-rates. So x_0 is assumed to be 0, i.e. $s_0(x) = s(x)$.

1) *Estimation of Edge Contrast*: From (16), we know that filtering of $s_0(x)$ by $f(x)$ does not influence contrast parameter c . Moreover, it is shown in [22] that for multipoint estimation, c can be estimated with greater accuracy and precision than w and b , even in the presence of noise, here the quantization noise. Thus, the initial estimated result \bar{c} from $s_1(x)$ can be used directly, as

$$\hat{c} = \bar{c}. \quad (19)$$

2) *Estimation of Edge Basis*: Quantization noise $q_n(x)$ in (16) may degrade the precision of the estimation of parameter b , since the computation of \hat{b} is based on the intensity value of the edge point which may be corrupted by the quantization noise $q_n(x)$. Therefore, a Gaussian filter $g_s(x; \sigma_s)$ is applied for smoothing $q_n(x)$ in $s_1(x)$ as

$$\begin{aligned} s_2(x) &= s_1(x) * g_s(x) \\ &= s(x; w_1, b, c) * g_s(x) + q_n(x) * g_s(x) \\ &\approx s(x; w_3, b, c) \end{aligned} \quad (20)$$

where $w_3 = \sqrt{w_1^2 + \sigma_s^2}$ and it is assumed that $q_n(x)$ and other noise have been averaged out by $g_s(x)$ with a proper choice of the spread parameter σ_s .

Theoretically, the filtering of $g_s(x)$ does not cause any shift to the edge center of the edge model. Furthermore, without considering $q_n(x)$ in $s_1(x)$, $g_s(x)$ also leaves the intensity value of the edge center unchanged, i.e. $s_1(0) = s_2(0)$. Then, after smoothing in (20), it is assumed that the value of the original

edge center $s_0(0)$ can be approximated by $s_2(0)$. Therefore, we regard the detected edge point $x = 0$ in (18) (when the appropriate conditions, as described in Section II-D, are met) as the edge center of the original signal $s_0(x)$, then b can be estimated by

$$\hat{b} = s_2(0) - \frac{\bar{c}}{2}. \quad (21)$$

3) *Estimation of Edge Width*: On account of low-pass filtering by $f(x)$, as shown in (16), some blurring distortion may be caused to the model parameter w . From (17), we can restore w by

$$\hat{w} = \frac{\bar{w}}{\lambda} \quad (22)$$

where λ is the widening coefficient and can be determined by our later experimental analysis.

Thus, the original edge-model parameters are able to be estimated from the coded signal. According to the definition of the edge model of (4), we can achieve model-based edge approximation for recovering original edge structure. Of course, the formulation of (16) is an approximation to characterized the degradation process of wavelet-based image coding, which has some errors influencing the post-processing results.

F. Error Analysis in the Compressed Signal

From (16), we know that the edge model in the compressed signal has suffered from two major errors: the modeling of zero phase low-pass filtering of $f(x)$ and the quantization noise $q_n(x)$. Both of them are discussed as follows, with respect to their influences in edge detection and model parameter estimation.

1) Influence of Modeling Error of $f(x)$:

a) *Edge localization*—: For a detected edge point in the coded signal, the error of edge localization may be due to the formulation of $f(x)$ in (15) being no longer in force. In this case, the edge reconstruction later around this edge point is implemented not so much for fidelity improvement but more for visual enhancement. This may happen often when the image is compressed at low bit-rates.

b) *Parameter estimation*—: If the modeling of (15) is valid and $q_n(x)$ is relatively small, the principal error now is that of parameter estimation of w , namely that of the widening factor λ in (17). In a 2-D image, due to the directional decomposition of DWT and the different rates of decaying spectrum shown in Fig. 2 of the edge model, the same high-frequency truncation may result in a different low-pass filtering effect on the edges with different directions or with different model parameters. It is difficult to develop a precise formulation for determining an exact widening coefficient λ for any given edge. Therefore, we try to determine an empirical setting for λ through experiments. We shall show that although one value of λ in the formulation of (16) may not be accurate for all edges in one coded image, the post-processing algorithm using such simplified characterization can still perform effectively for most tested images.

2) Influence of Quantization Noise $q_n(x)$:

a) *Edge detection and localization*: The performance of a filter in revealing an edge can be evaluated by Canny's signal-to-

noise criterion Ω and localization criterion Λ [23], from which van Beek deduced those criteria for the Gaussian smoothed step edge detected with Canny detector as follows:

$$\Omega_1 = \frac{c}{\sigma_n} \sqrt{\frac{2\sigma_d^3}{(w^2 + \sigma_d^2)\sqrt{\pi}}} \quad (23)$$

and

$$\Lambda_1 = \frac{c}{\sigma_n} \sqrt{\frac{4\sigma_d^5}{3(w^2 + \sigma_d^2)^3\sqrt{\pi}}} \quad (24)$$

with σ_n the standard deviation of the noise. Here we consider σ_n as the standard deviation of quantization noise $q_n(x)$ introduced by zero-tree quantization of wavelet coefficients, and σ_d is the filter scale of edge detection. A large value of scale σ_d in (23) is necessary in order to smooth the quantization noise $q_n(x)$ and reach higher SNR's Ω_1 , but the performance of localization Λ_1 would suffer. Thus, an appropriately compromised σ_d of edge detector should be set.

b) Parameter estimation: The above two criteria are concerned with the multipoint-model parameter estimation which is conducted based on the outputs of edge detection. In order to determine the accuracy of multipoint parameter estimation, another SNR criterion is introduced in [22], which is discerned from one another in the response of edge detection under noisy circumstance and can show how well the difference values of the same response used in the estimation. Thus, Van Beek defined the ‘‘difference signal-to-noise’’ as

$$\Omega_2 = \Omega_1 |1 - e^{-(a^2/2(w^2 + \sigma_d^2))}|. \quad (25)$$

For a Gaussian smoothed-edge model, $\Omega_2 \leq \Omega_1$ for all σ_d . Since $q_n(x)$ lowers the performance of edge detection Ω_1 , multipoint estimation seems to be sensitive to the quantization noise. Therefore, we need a suitable setting of σ_d to keep the precision of model parameter estimation in coded images. In our experiments, it was found that $\sigma_d \in (1.3, 1.6)$ is suitable for most images coded by wavelet-based coding using zero-tree quantization at low bit-rates.

In practice, the different errors above may introduce different influences on the result of edge reconstruction. The error of degradation formulation by $f(x)$ is mainly related to the nature of image post-processing, preferring image enhancement or image restoration. That of quantization noise may affect the quality of edge reconstruction in a certain meaning.

By now, we study the behavior of the lossy edges in the compressed signal by developing the original edge model to the case of the coded signal. The associated parameter estimation scheme is carried out for estimating the original model parameters from the coded signal. Then according to the definition of the edge model (4), the approximation of the original edge structure can be obtained. All the results above can be extended to the 2-D case directly.

III. EDGE-RECONSTRUCTION ALGORITHM

In an image coded by wavelet-based coding at low bit-rates, edge distortions happen mainly within narrow strips, namely

edge region, along edge curves. For efficient image post-processing, the edge region needed to be reconstructed should be determined firstly. From the analysis in Section II-C, we know that two artifacts in the edge region can be characterized by the degradation model given by (16). In order to recover lossy edges with the reproduction of edge sharpness and the reduction of ringing effects, we introduced two operations follows.

A. Two Operations

In the proposed algorithm, we develop two operations, *model-based edge approximation* and *Gaussian smoothing*, which are related to the two additional terms in the lossy-edge model and aimed at the suppression of the two artifacts. An important question is now, for a pixel in the edge region to be reconstructed, how to obtain a reasonable balance between the two operations. To this end, we need to understand the characteristics of the errors embedded in the two operations. The error of model-based approximation mainly results from that of model parameter estimation, and Gaussian filtering may cause some intensity deviations to the filtered signal. We will discuss this problem under 1-D case as follows.

Given an edge signal $s_0(x; w, b, c)$ defined by (4) and its coded version $s_1(x; w_1, b, c)$ with $w_1 = \lambda w$, let the errors between the estimated parameters \hat{w} , \hat{b} and \hat{c} and the original ones, w , b and c be Δw , Δb , and Δc , respectively, i.e.

$$\begin{aligned} \hat{w} &= w + \Delta w \\ \hat{b} &= b + \Delta b \\ \hat{c} &= c + \Delta c. \end{aligned}$$

Then $\hat{s}_0(x)$, the model-based approximation of $s_0(x)$, is given by

$$\hat{s}_0(x; b, c, w) = (b + \Delta b) + \frac{c + \Delta c}{2} \cdot \left(1 + \operatorname{erf}\left(\frac{x}{(w + \Delta w)\sqrt{2}}\right)\right).$$

The magnitude of the approximation error is

$$e(x) = |\hat{s}_0(x) - s_0(x)| \leq e_0 + e_1(x) \quad (26)$$

where

$$e_0 = \left| \Delta b + \frac{\Delta c}{2} \right| \quad (27)$$

and

$$e_1(x) = \left| \frac{c + \Delta c}{2} \operatorname{erf}\left(\frac{x}{(w + \Delta w)\sqrt{2}}\right) - \frac{c}{2} \operatorname{erf}\left(\frac{x}{w\sqrt{2}}\right) \right|. \quad (28)$$

Since the values of w are mainly among (0.5, 1.5) and for most cases $\Delta w < w$, $e_1(x)$ can be approximated by

$$e_1(x) \approx \left| \frac{\Delta c}{2} \operatorname{erf}\left(\frac{x}{w\sqrt{2}}\right) \right|. \quad (29)$$

Therefore, we can see that the validity of model-based approximation decreases as x increases. In other words, the model-

based approximation may not be credible for pixels far away from edge points.

As stated before, the model-based approximation enables us to recover edge structures, and Gaussian filter is applied for smoothing the quantization noise around edges. However, Gaussian filtering, at the same time, introduces intensity deviation to the filtered signal, which happens mostly among the transition region of the signal. That means the pixels far away from edge points bear fewer deviation and are closer to the original values compared with those among the transition regions carrying sharp intensity changes. With these considerations, we develop a model-based edge-reconstruction algorithm as follows.

B. Algorithm

The proposed edge-reconstruction algorithm consists of three steps which are *selection of the edge region*, *model-based edge reconstruction* and *projection operation in the wavelet domain*. Let \mathcal{DWT} and \mathcal{IDWT} be the DWT pair, and $\lceil \cdot \rceil_{T_q}$ denotes the zero-tree quantization operator with quantization threshold T_q .

1) *Selection of the Edge Region*: Edges of 2-D images are often not isolated but belong to some curves which generally are the boundaries of the image structure. Usually, long edge curves are more important for human perception compared with short ones. Therefore, edges are reconstructed along the edge curves of significant length.

Let Φ be an original image and $\tilde{\Phi}$ its coded version. The quantized wavelet coefficient array of $\tilde{\Phi}$ is denoted by W where most coefficients are zero. A pixel at (x, y) in $\tilde{\Phi}$ is denoted as $p(x, y)$, and the distance between $p(x_1, y_1)$ and $p(x_2, y_2)$ is defined by

$$D(p(x_1, y_1), p(x_2, y_2)) = \sqrt{(x_1 - x_2)^2 + (y_1 - y_2)^2}.$$

Let I_e^j be the set which contains edge points of the j th edge curve detected in $\tilde{\Phi}$, and $L(I_e^j)$ be the length of curve I_e^j . Suppose there are n curves in $\tilde{\Phi}$. We define two sets, I_E and I_R , as follows:

$$\begin{aligned} I_E &= \{p(x, y) | p(x, y) \in I_e^j, L(I_e^j) > L_0, \text{ with } 1 \leq j \leq n\} \\ I_R &= \{p(x, y) | D(p(x, y), p(x_e, y_e)) \leq D_0, p(x_e, y_e) \in I_E \\ &\quad \text{and } p(x_e, y_e) = \arg_{p(x_e, y_e)} \min D(p(x, y), p(x_e, y_e))\} \end{aligned}$$

where L_0 and $D_0 = \sqrt{8}$ are two thresholds for length filtering and modulus thresholding, respectively. I_E contains edge points of the edge curves of significant length. I_R is the edge region to be recovered.

2) *Model-Based Edge Reconstruction*: For a certain pixel $p(x, y) \in I_R$, its intensity value is denoted by $\tilde{\Phi}(x, y)$ and its model-based approximation $\Theta(x, y)$ is given by

$$\Theta(x, y) = \hat{b}_e + \frac{\hat{c}_e}{2} \left(1 + \operatorname{erf} \left(\frac{l}{\hat{w}_e} \right) \right) \quad (30)$$

where $l = D(p(x, y), p(x_e, y_e))$ and $p(x_e, y_e) \in I_E$ is the nearest edge point to $p(x, y)$; \hat{c}_e , \hat{b}_e and \hat{w}_e are the estimated model parameters of the original image associated with pixel $p(x_e, y_e)$. $\Theta(x, y)$ is mainly used for deblurring the lossy edges. In practice, the value of $\Theta(x, y)$ may not be close to the original intensity of $p(x, y)$. This is due to the lossy approximation of

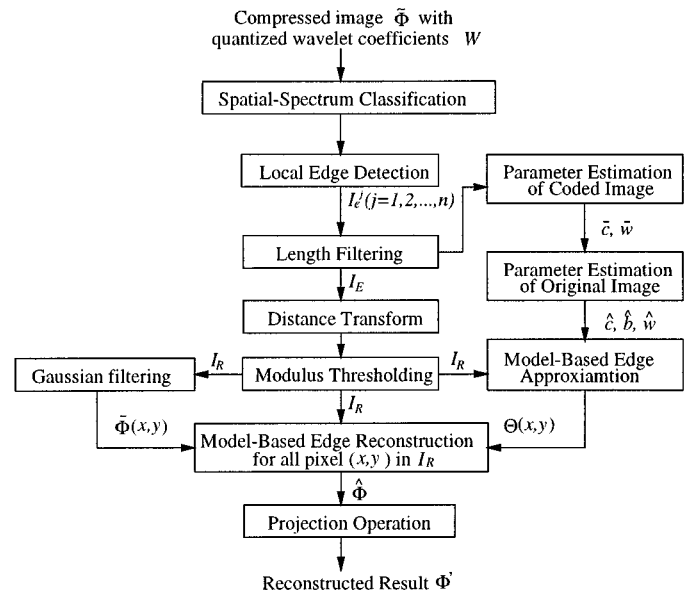


Fig. 4. The schematic diagram of model-based edge reconstruction.

the edge model to the real edges and the degraded precision of multipoint model parameter estimation shown in Section III-A. However, $\Theta(x, y)$ provides an eye-pleasing intensity tendency for each $p(x, y) \in I_R$. This is attributed to the regularized edge structure defined by the edge model. In order to measure the reliability of the approximation for edge reconstruction, according to the analysis above, we construct a confident function Γ as

$$\Gamma(l) = e^{-l \cdot \alpha}, \text{ with } \alpha \geq 0 \quad (31)$$

where l is the distance between the pixel to be performed edge reconstructed and its nearest edge point, and α is an empirical factor.

On the other hand, in the coded image $\tilde{\Phi}$, the intensities of the pixels in I_R contain quantization noise which is exhibited as the ringing effect around edge curves. A 2-D Gaussian filter $g_s(x, y; \sigma_s)$ is adopted with $\sigma_s = 1.0$ for reducing this noise, since a small spread parameter σ_s adapts to a rapidly-varying signal better than a large one [24]. This Gaussian smoothing operation coincides with that used for estimating model parameter b in (21). The filtered result of each pixel $p(x, y) \in I_R$ is denoted by

$$\bar{\Phi}(x, y) = \tilde{\Phi} * g_s(x, y). \quad (32)$$

Since the deviation of $\bar{\Phi}(x, y)$ introduced by Gaussian filtering may decrease with the increase of l , as shown in Section III-A, we weight $\bar{\Phi}(x, y)$ by $1 - \Gamma(l)$.

Both $\Theta(x, y)$ of (30) and $\bar{\Phi}(x, y)$ of (32), which target two different artifacts existing at edges are incorporated into the edge reconstruction of $p(x, y)$. We introduce a reconstruction model with $\Gamma(l)$ adjusting the balance between them as follows:

$$\hat{\Phi}(x, y) = \Gamma(l)\Theta(x, y) + (1 - \Gamma(l))\bar{\Phi}(x, y). \quad (33)$$

By tuning α in (31), the influences of two operations on each reconstructed pixel $p(x, y)$ can be adjusted according to its dis-

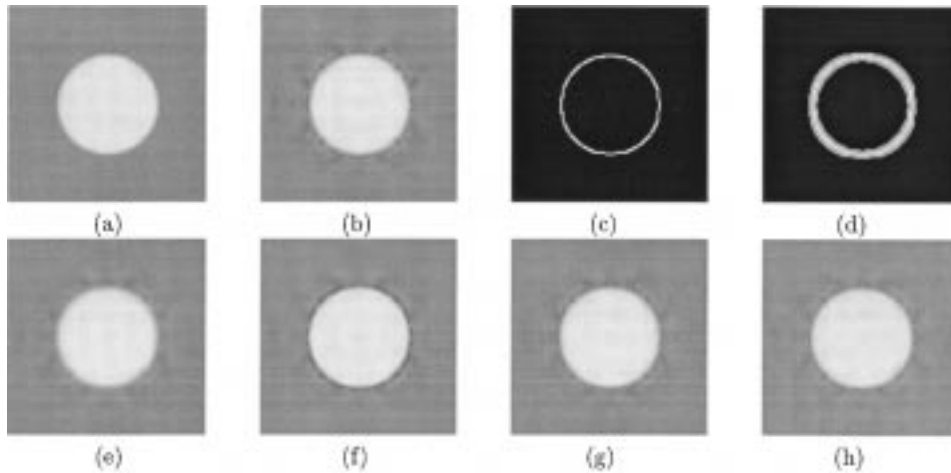


Fig. 5. Edge reconstruction results for a synthetic image. (a) Original image Φ . (b) Coded image $\bar{\Phi}$ (40.22 dB, 0.10 bpp). (c) Result of edge detection I_E . (d) Edge region I_R to be reconstructed. (e) Gaussian smoothed version $\tilde{\Phi}$. (f) Model-based edge approximation Θ . (g) Initial revised version $\hat{\Phi}$. (h) Reconstructed image Φ' (PSNR gain = 1.12 dB).

TABLE I
MODEL PARAMETER ESTIMATION OF EDGE CONTRAST c

	$w_1 = 0.5$		$w_2 = 0.8$		$w_3 = 1.1$		$w_4 = 1.4$		$w_5 = 1.7$		$w_6 = 2.0$	
	$m(c)$	$sd(c)$										
Φ_n	97.3	11.9	97.5	9.3	98.0	7.0	97.9	5.6	98.1	4.5	98.5	3.1
$\tilde{\Phi}_n$	99.8	8.3	97.5	7.6	96.6	8.9	99.4	7.5	102.1	10.4	106.1	13.0

TABLE II
MODEL PARAMETER ESTIMATION OF EDGE BASIS b

	$w_1 = 0.5$		$w_2 = 0.8$		$w_3 = 1.1$		$w_4 = 1.4$		$w_5 = 1.7$		$w_6 = 2.0$	
	$m(b)$	$sd(b)$										
Φ_n	96.6	15.4	99.9	13.8	99.8	12.9	99.8	10.1	100.3	9.5	100.0	7.8
$\tilde{\Phi}_n$	101.2	17.7	99.1	14.6	101.1	13.9	101.1	11.9	97.4	10.7	110.0	11.8
$\hat{\Phi}_n$	98.3	8.5	97.4	7.5	97.0	8.6	99.3	7.4	101.7	10.2	105.8	11.1

tance to the nearest edge point. For an image, we may adjust α to attain the highest PSNR gain. However, if we consider the image fidelity as a less important factor, then a smaller α , which will strength the effect of model-based reconstruction, can be chosen to obtain a sharper edge structure. Thus, α provides a trade-off between visual enhancement and PSNR improvement for the reconstructed image $\hat{\Phi}$.

3) *Projection Operation in the Wavelet Domain*: After the edge reconstruction of (33), we require a projection operation defined as follows to ensure that the reconstructed image $\hat{\Phi}$ exists in the same quantization space with that of the coded image $\bar{\Phi}$

$$W'(i, j) = \begin{cases} W(i, j), & \text{if } W(i, j) \neq 0 \\ \pm T_q, & \text{if } W(i, j) = 0 \text{ and } |\hat{W}(i, j)| > T_q \\ \hat{W}(i, j), & \text{otherwise} \end{cases}$$

where $\hat{W} = DWT(\hat{\Phi})$ and $\hat{\Phi}$ is obtained from (33); (i, j) is the coordinate of wavelet coefficients; W is the zero-tree thresholded wavelet coefficient array of the coded image $\bar{\Phi}$. T_q is the quantization threshold of W , which can be deduced from the smallest magnitude of non-zero wavelet coefficients in W ; W' is the reconstructed wavelet coefficient array. The operation of $\Phi' = IDWT(W')$ gives the final reconstructed image Φ' .

C. Implementation

The schematic diagram of the proposed algorithm is shown in Fig. 4. In order to speed up edge detection, we can narrow the detected region through spatial-spectrum classification of image blocks by using the spatial characteristic of wavelet coefficients [25]. Thus, edge detection is conducted locally where there may be some existing edges, and the combination of local edge detection results produces a complete result, namely $I_e^j (j = 1, 2, \dots, n)$ for n edge curves. Then, after length filtering, the set of edge points in edge curves of significant length I_E can be determined, from which the edge region I_R to perform edge reconstruction can be selected by the distance transform [26] of I_E followed by modulus thresholding. Every pixel in I_R is reconstructed according to the reconstruction model in (33) and the initially revised image is denoted as $\hat{\Phi}$, from which the last reconstruction result Φ' is obtained by the projection operation in the wavelet domain.

Here, we present the implementation procedure of our algorithm in Fig. 5 by processing a synthetic image coded by a wavelet-based codec, SPIHT [12] at 0.1 bpp, PSNR = 40.22 dB shown in Fig. 5(a), which has invariant model parameters around the circle edge, i.e., $w = 1.0$, $c = 100$ and $b = 100$. The step-by-step results can be obtained from Fig. 5(b)–(h). The last edge-reconstructed result is shown in

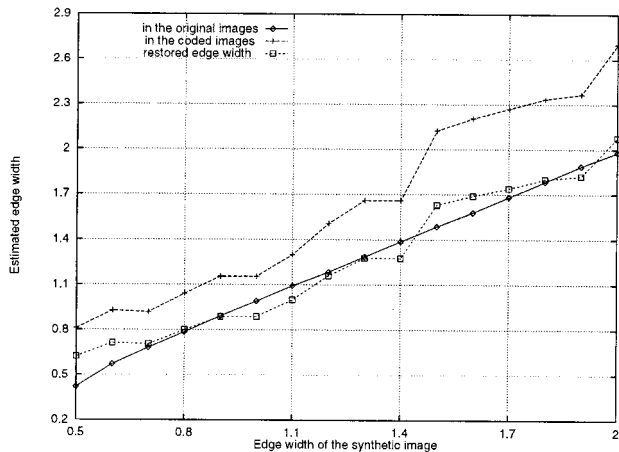


Fig. 6. Determination of λ for restoring edge width w .

Fig. 5(h), whose PSNR and subjective quality have been improved. From Fig. 5(d), we know that only a very small part of the lossy image is post-processed due to the existence of edges there. However, the improvements on visual perception and image fidelity are notable. Hence, the necessity and desirability of edge reconstruction for low bit-rate compressed images are manifested.

IV. EXPERIMENTAL RESULTS

The experiments of this work have been applied primarily to the images coded by the efficient wavelet-based codec—SPIHT [12].¹ We expect that the proposed approach is also applicable to other codecs using zero-tree quantization, such as SFQ [13].

A. Setting Algorithm Parameters

The values of two important factors in the proposed algorithm, λ and α need to be determined for the edge model and the reconstruction model discussed above. The two factors have different influences on the result of post-processing. λ shows the sensitiveness of post-processing and α affects the strength of model-based edge reconstruction. Since λ is closely related to the edge model, we shall determine its setting by the experimental analysis based on synthetic images which contains edges in all directions and of different edge width w . On the other hand, the value of α reflects the precision of the model-based approximation with respect to low bit-rate image coding; therefore, we shall determine its value based on a number of standard images coded at low bit-rates.

1) *Model Parameter Estimation and Setting λ* : λ is the widening factor to model the low-pass filtering effect due to zero-tree quantization and is related to the bit-rate and the original edge model parameters. In order to simplify our investigation, we have introduced some preconditions for the experimental synthetic images.

Condition 1: The values of edge width should be in the range of (0.5,2.0), since the majority of edges in most images is within such range [22].

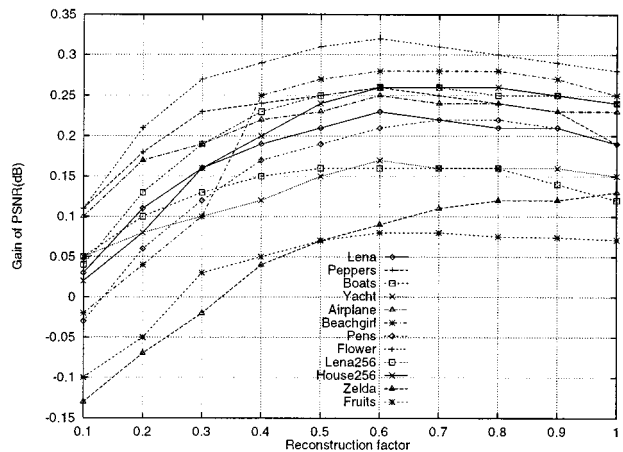


Fig. 7. Determination of α for edge reconstruction.

Condition 2: The value of edge contrast $c = 100$ is adopted for the edges in all tested synthetic images, since it is a representative value for most images.

Condition 3: We apply $T_q = 32$ to the quantization of the wavelet coefficients of the original synthetic images to obtain their coded versions at low bit rates, since for most images coded by SPIHT at low bit rates, the values of T_q are 16, 32, or 64.

Though the above simplified conditions may not have provided us the optimal setting of λ , we can still obtain an empirical value of λ which enables effective post-processing for most images. Consider synthetic images $\Phi_n (n = 1, 2, \dots)$ similar to Fig. 5(a) with $c = b = 100$ and different values of edge width ($w_n = 0.5 \sim 2.0$) along the circle edge. For each image $\Phi_n (n = 1, 2, \dots)$, we calculate $W_n = [DWT(\Phi_n)]_{T_q}$ with $T_q = 32$, and let its coded version be $\tilde{\Phi}_n = IDWT(W_n)$. Then, we compute the estimated values of model parameters for each $\tilde{\Phi}_n (n = 1, 2, \dots)$ using $\sigma_d = 1.5$ in (5) for edge detection. For comparison, the parameter estimation is also developed on the original image Φ_n . Moreover, the parameter b is estimated from the image $\bar{\Phi}_n$, which is the Gaussian smoothed version of $\tilde{\Phi}_n$ filtered by $g(x, y; \sigma_s)$ with $\sigma_s = 1.0$. The means and standard deviations of the estimated parameters c and b are computed and listed in Tables I and II, respectively. It is shown that wavelet-based image coding introduces little bias on edge model parameters, c and b . However, we need to restore w according to (22). Fig. 6 plots the edge width estimated using (11) against the original edge width for the original and coded images, Φ_n and $\tilde{\Phi}_n (n = 1, 2, \dots)$. Tables I and II show that for images coded with $T_q = 32$, the mean values of the estimated c and b are about the same for the original and coded images. In addition, Gaussian smoothing by $g(x, y; \sigma_s)$ improves the estimation precision of parameter b . Moreover, for the estimated w , we should restore it by λ according to (22). Fig. 6 suggests that $\lambda = 1.3$. For a coded image, the optimal (maximum PSNR) value of λ , is normally between 1.2 and 1.6, depending on the bit-rate and the image content.

2) *Edge Reconstruction and Setting α* : The factor α in (31) can be determined through extensive experiments on many standard images coded at low bit-rates and using PSNR as a criterion. Here we have used twelve images. Ten 512×512 images coded at 0.1 bpp and two 256×256 images coded at 0.2 bpp

¹ The software and documentation which are copyrighted may be accessed online. Available: <http://www.cipr.rpi.edu/research/SPIHT/>

TABLE III
EDGE RECONSTRUCTED RESULTS FOR IMAGES (512×512 , 8 bpp)

bit-rates (bpp)	Lena		Peppers		Flower		Monarch	
	PSNR(dB)	Gain	PSNR(dB)	Gain	PSNR(dB)	Gain	PSNR(dB)	Gain
0.20	33.26	+0.11	32.83	+0.10	36.25	+0.06	30.26	+0.35
0.15	32.02	+0.13	31.68	+0.13	34.78	+0.32	29.00	+0.50
0.10	30.45	+0.23	30.10	+0.26	32.34	+0.32	27.11	+0.47
0.08	29.60	+0.25	29.12	+0.23	31.16	+0.34	26.13	+0.44

TABLE IV
EDGE RECONSTRUCTED RESULTS FOR IMAGES (256×256 , 8 bpp)

bit-rates (bpp)	Lena256		House		Camera		Tree	
	PSNR(dB)	Gain	PSNR(dB)	Gain	PSNR(dB)	Gain	PSNR(dB)	Gain
0.25	30.00	+0.04	33.08	+0.14	28.00	+0.03	26.03	+0.25
0.20	28.18	+0.18	32.12	+0.20	27.17	+0.10	25.17	+0.25
0.15	27.12	+0.25	30.82	+0.25	25.96	+0.12	23.92	+0.23
0.10	25.56	+0.23	29.11	+0.33	24.54	+0.18	22.49	+0.24



Fig. 8. Result for Lena (512×512 , 8 bpp). (a) Coded image (30.22 bpp, 0.10 bpp). (b) Reconstructed image (30.45 dB, +0.23 dB).



Fig. 9. Result for Peppers (512×512 , 8 bpp). (a) Coded image (29.84 bpp, 0.10 bpp). (b) Reconstructed image (30.10 dB, +0.26 dB).

were employed to determine α , as illustrated in Fig. 7. It is shown that $\alpha = 0.6$ is near optimal for most images in this set. But the precise setting of α is image and bit-rate dependent. It is because different images may coincide with the edge model

in different degree and the bit-rate of a coded image will influence the precision of model parameter estimation. In general, $\alpha \in (0.5, 0.7)$ gives the best PSNR gain for most images coded at low bit-rates.



Fig. 10. Result for Flower (512×512 , 8 bpp). (a) Coded image (32.02 bpp, 0.10 bpp). (b) Reconstructed image (32.34 dB, +0.32 dB).



Fig. 11. Result for Monarch (512×512 , 8 bpp). (a) Coded image (26.64 bpp, 0.10 bpp). (b) Reconstructed image (27.10 dB, +0.46 dB).

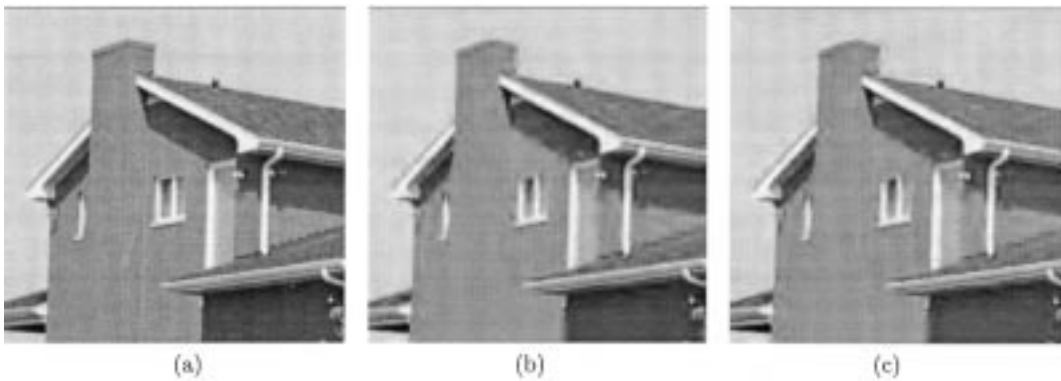


Fig. 12. Result for House (256×256 , 8 bpp). (a) Original image. (b) Coded image (30.57 bpp, 0.15 bpp). (c) Reconstructed image (30.82 dB, +0.25 dB).

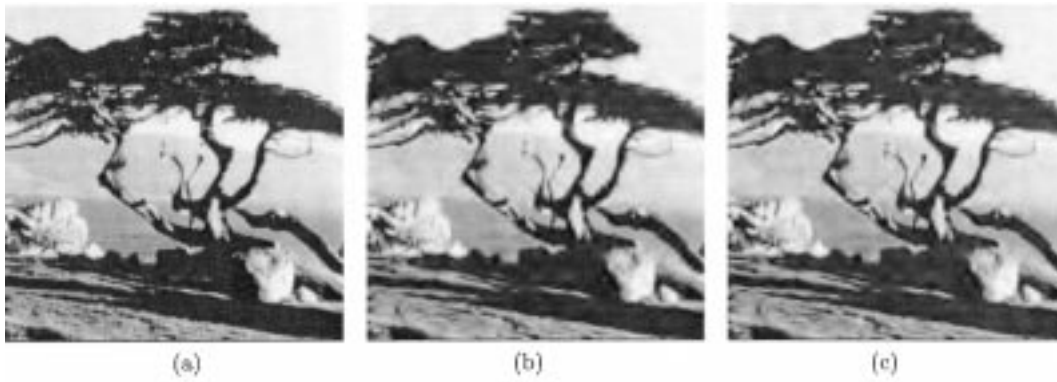


Fig. 13. Result for Tree (256×256 , 8 bpp). (a) Original image. (b) Coded image (25.78 bpp, 0.25 bpp). (c) Reconstructed image (26.03 dB, +0.25 dB).

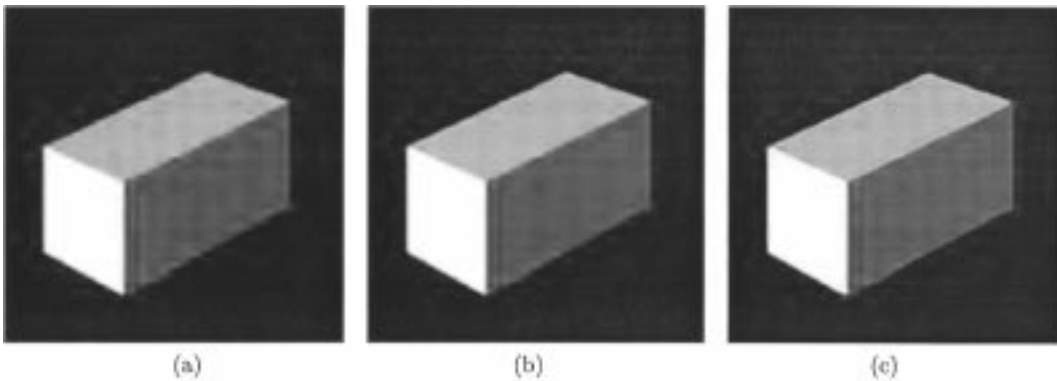


Fig. 14. Result for Box (256×256 , 8 bpp). (a) Coded image (0.06 bpp). (b) Reconstructed with $\alpha = 0.6$ (PSNR gain = 1.05 dB). (c) Reconstructed with $\alpha = 0.2$ (PSNR gain = 0.65 dB).

B. Results

We apply the edge reconstruction scheme to twelve standard images coded by SPIHT at low bit-rates. In all experiments, we used $\lambda = 1.3$ and $\alpha = 0.6$. Tables III and IV show the improvements of image fidelity (PSNR) for the images coded at low bit-rates. Figs. 8–13 illustrate that the visual quality of the coded images is also improved. Around edges, not only the ringing effects are reduced, edges also appear to be sharper. Moreover, if one emphasizes the edge enhancement of the reconstructed result by choosing $\alpha < 0.5$, images of sharp edges with little or no PSNR gain will result. Fig. 14 shows two versions of edge reconstruction for a coded synthetic image *Box* with different setting of the reconstruction factor α . The computation time of the proposed algorithm depends on the amount of edges exist in an image. For normal images of 512×512 , like *Lena* and *Pep-pers*, the computation time is about 20 s on a 200-MHz Pentium computer.

In general, there are two factors affecting the efficiency of the proposed post-processing algorithm: the bit rate and image content. For those images with fewer noticeable edge structures, such as *Fruits* and *Zelda*, or images with abundant random textures, such as *Baboon* and *Bridge*, the proposed method may not be able to improve the PSNR or visual quality significantly. Moreover, we have simplified our problems by assuming that images coded at different bit rates bear the same edge degradation. In fact, for images coded at very low bit-rates, serious edge distortions, such as shifting or vanishing of edges, will result

and the endeavor of the proposed edge reconstruction may be in vain. On the other hand, if the coded image carries less edge distortion or there is not enough edge degradation, the profit to be gained from the edge reconstruction is also negligible. Therefore, the proposed method is more effective for images which have obvious, but not deadly, edge distortion. Experiments also show that the visual quality and PSNR of the reconstructed image will not deteriorate and remains at the original level if the proposed post-processing cannot provide an improvement. This is probably due to the fact that, in this case, the proposed post-processing algorithm will perform little operation on the image.

V. CONCLUSIONS

A new technique for image post-processing has been presented which is able to perform edge reconstruction for images coded by wavelet-based coding at low bit-rates. The image quality can be improved in terms of both PSNR and visual perception. The proposed approach has the following two features.

- 1) The edge model is deterministic and the edge-degradation model is simple and direct. These allow a straightforward implementation of the proposed post-processing algorithm.
- 2) The parameterized reconstruction model allows a flexible tradeoff between visual enhancement and PSNR gain for the reconstructed image.

The key in the proposed method is the degradation modeling of edges in an image, where the edge model also plays an important role. It is shown that the proposed algorithm is promising in stretching the performance of wavelet-based coding using zero-tree quantization at low bit-rates.

ACKNOWLEDGMENT

The authors are thankful to Prof. X. Zhu of Tsinghua University and Dr. J. Liu of The Chinese University of Hong Kong for their helpful comments.

REFERENCES

- [1] Y. Yang, N. P. Galatsanos, and A. K. Katsaggelos, "Projection-based spatially adaptive reconstruction of block-transform compressed images," *IEEE Trans. Image Processing*, vol. 4, pp. 896–908, July 1995.
- [2] —, "Regularized reconstruction to reduce blocking artifacts to the block discrete cosine transform compressed images," *IEEE Trans. Circuits Syst. Video Technol.*, vol. 3, pp. 421–432, Dec. 1993.
- [3] S. W. A. and S. W. Gersho, "Improved decoder for transform coding with application to the JPEG baseline systems," *IEEE Trans. Commun.*, vol. 40, pp. 251–254, Feb. 1992.
- [4] R. L. Stevenson, "Reduction of coding artifacts in transform image coding," in *Proc. ICASSP'93*, vol. V, 1993, pp. 401–404.
- [5] R. Rosenblatz and A. Zakhor, "Iterative procedure for reduction of blocking effects in transform image coding," in *IEEE Trans. Circuits Syst. Video Technol.*, vol. 2, Mar. 1992, pp. 91–95.
- [6] J. D. McDonnell, R. N. Shortern, and A. D. Fagan, "Postprocessing of transform coded images via histogram-based edge classification," *J. Electron. Imaging*, vol. 6, no. 1, 1997.
- [7] J. Luo, C. Chen, and K. J. Park, "On the application of gibbs random field in image processing: Form segmentation to enhancement," *J. Electron. Imaging*, vol. 4, no. 2, pp. 187–198, Apr. 1995.
- [8] W. E. Lynch, A. R. Reibman, and B. Liu, "Post processing transform coded images using edges," in *Proc. ICASSP'95*, vol. IV, 1995, pp. 2323–2326.
- [9] Z. Fan and R. Eschbach, "JPEG decompression with reduced artifacts," in *Proc. SPIE 1996 Symp. Image and Video Compression*, vol. 2186, Feb. 1996, pp. 50–55.
- [10] T. P. O'Rourke and R. L. Stevenson, "Improved image decompression for reduced transform coding artifacts," *IEEE Trans. Circuits Syst. Video Technol.*, vol. 5, pp. 490–499, Dec. 1995.
- [11] J. M. Shapiro, "Embedded image coding using zerotrees of wavelet coefficients," *IEEE Trans. Signal Processing*, vol. 41, no. 12, pp. 3445–3463, 1993.
- [12] A. Said and W. A. Pearlman, "A new fast and efficient image codec based on set partitioning in hierarchical trees," *IEEE Trans. Circuits Syst. Video Technol.*, vol. 6, pp. 243–250, 1996.
- [13] Z. Xiong, K. Ramchandran, and M. T. Orchard, "Wavelet packet image coding using space-frequency quantization," *IEEE Trans. Image Processing*, vol. 6, pp. 677–693, May 1997.
- [14] S. M. LoPresto, K. Ramchandran, and M. T. Orchard, "Image coding based on mixture modeling of wavelet coefficients and a fast estimation-quantization framework," presented at the IEEE DCC'97, 1997.
- [15] C. W. Kok and T. Q. Nguyen, "Document image compression by sub-band system," *Preprint*, 1996.
- [16] J. Luo, C. Chen, and K. J. Parker, "Image enhancement for low bit rate wavelet-based compression," in *Proc. ISCAS'97*, 1997, pp. 1081–1084.
- [17] I. Linares, "Optimal PSNR estimated spectrum adaptive postfilter for DCT coded images," in *Proc. ICASSP'95*, vol. IV, 1995, pp. 2387–2380.
- [18] A. K. Katsaggelos, *Digital Image Restoration*. New York: Springer-Verlag, 1991.
- [19] A. Narayan and J. F. Doherty, "Convex projections based edge recovery in low bit rate VQ," *IEEE Signal Processing Lett.*, vol. 3, pp. 97–99, Apr. 1996.
- [20] K. Sauer, "Enhancement of low bit-rate coded image using edge detection and estimation," *Comput. Vision, Graphics, Image Processing*, vol. 53, no. 1, pp. 52–62, 1991.
- [21] W. K. Carey, D. B. Chuang, and S. S. Hemami, "Regularity-preserving image interpolation," in *Proc. ICIP'97*, 1997, pp. 901–904.
- [22] P. J. L. van Beck, "Edge-Based Image Representation and Coding," Ph.D. dissertation, Delft University of Technology, The Netherlands, 1995.
- [23] J. Canny, "A computational approach to edge detection," *IEEE Trans. Pattern Anal. Machine Intell.*, vol. PAMI-8, pp. 679–698, 1986.
- [24] G. Deng and L. W. Cahill, "An adaptive Gaussian filter for noise reduction and edge detection," presented at the IEEE Conf. Record. Nuclear Science Symposium and Medical Imaging Conference.
- [25] H. Jafarkhani and N. Farvardin, "Adaptive image coding using spectral classification," *Preprint*.
- [26] G. Borgefors, "Distance transforms in arbitrary dimensions," *Comput. Vision, Graphics, Image Processing*, vol. 27, pp. 321–345, 1984.



Guoliang Fan (S'97) was born in Xi'an, China, in 1971. He received the B.E. degree in automation engineering from Xi'an University of Technology, China, and the M.S. degree in computer engineering from Xidian University, China, in 1993 and 1996, respectively. He is presently working toward the Ph.D. degree in the Department of Electrical and Computer Engineering, University of Delaware, Newark, DE.

His research interests include image compression, image enhancement, and statistical signal and image processing.

Mr. Tan was the recipient of the First Prize of 1997 IEEE Hong Kong Section Postgraduate Student Paper Contest, and he was also awarded the First Prize of 1997 IEEE Region 10 Postgraduate Student Paper Contest.



Wai-Kuen Cham (S'77–M'79–SM'91) graduated from the Chinese University of Hong Kong in 1979 in electronics. He received the M.Sc. and Ph.D. degrees from Loughborough University of Technology, U.K., in 1980 and 1983, respectively.

From 1984 to 1985, he was a Senior Engineer with Datacraft Hong Kong Limited and a Lecturer in the Department of Electronic Engineering, Hong Kong Polytechnic. Since May 1985, he has been with the Department of Electronic Engineering, the Chinese University of Hong Kong. His research interests include image coding, image processing and Chinese character recognition.